A Study of Photo-Thermoelastic Wave in Semiconductor Materials With Spherical Holes Using Analytical-numerical Methods

Faris S. Alzahrani
King Abdulaziz University Faculty of Sciences
Ibrahim Abbas (ibrabbas7@yahoo.com)
Department of mathematics, Faculty of Science, Sohag University, Sohag, Egypt
https://orcid.org/0000-0001-9595-439X

Research Article

Keywords: Finite difference method, Semiconductor material, Laplace transforms, spherical cavity, eigenvalues scheme

Posted Date: March 22nd, 2021

DOI: https://doi.org/10.21203/rs.3.rs-312019/v1

A Study of photo-thermoelastic wave in semiconductor materials with spherical holes using analytical-numerical methods

Faris S. Alzahrani[a] and Ibrahim A. Abbas[a,b1]

[a]Department of Mathematics, Faculty of Science, King Abdulaziz University, Jeddah, Saudi Arabia

[b]Department of mathematics, Faculty of Science, Sohag University, Sohag, Egypt.

E-mail: falzahrani1@kau.edu.sa & ibrabbas7@yahoo.com & ibrabbas7@science.sohag.edu.eg

Abstract

Analytical and numerical solutions are two basic tools in the study of photothermal interaction problems in semiconductor medium. In this paper, we compare the analytical solutions with the numerical solutions for thermal interaction in semiconductor mediums containing spherical cavities. The governing equations are given in the domain of Laplace transforms and the eigenvalues approaches are used to obtained the analytical solution. The numerical solutions are obtained by applying the implicit finite difference method (IFDM). A comparison between the numerical solutions and analytical solution are presented. It is found that the implicit finite difference method (IFDM) is applicable, simple and efficient for such problems.

Keywords: Finite difference method; Semiconductor material; Laplace transforms; spherical cavity; eigenvalues scheme.

Nomenclature

$N = n - n_o, n_o$	the carrier concentration at equilibrium,
$\gamma_n = (3\lambda + 2\mu)d_n, d_n$	the electronic deformation coefficient,
$\delta = \frac{\partial n_o}{\partial T}$	the coupling parameter of thermal activation
K	the thermal conductivity
$\gamma_t = (3\lambda + 2\mu)\alpha_t, \alpha_t$	the linear thermal expansion coefficients
c_e	the specific heat at constant strain,
τ	the lifetime of photo-generated carrier,
σ_{ij}	the components of stresses,

[1] Ibrahim Abbas, ibrabbas7@yahoo.com & ibrabbas7@science.sohag.edu.eg

D_e	the carrier diffusion coefficient,
λ, μ	the Lame's constants,
$T = T^* - T_o, T^*$	the variations of temperature
T_o	the reference temperature
t	the time
t_f	the final value of time
x_f	the final value of length
s_b	the speed of recombination on the surface
u_i	the displacement components
ρ	the density of material
T_1	the constant temperature
Ω	the exponent of the decayed heat flux

1 Introduction

In the surrounding nature, many materials are very important in industry especially, these materials have many applications in renewable energy. The semiconductor materials exist in abundance in the surrounding nature which have great economic importance in solar cells industry. When the semiconductor media are exposed to a focus of laser beams or a beam of sunlight, the surface electrons at free surface are thermally exited and they will be vibrated due to the thermal effect of laser beams. In this case, the electrons and holes will transport from one position to another and the free carriers photo-excited appearing with a weak electrical current. On the other hand, the recombination processes during the photo-excited processes will be taken into account between the electrons (carrier density (plasma)) and holes. Much effort has been made for generalized theories of thermoelasticity in solving thermoelastic models instead of the classical decoupled and coupled theory of thermoelasticity. For decoupled thermoelasticity, the absence of any term reflecting elasticity in the thermal conduction equation does not appear to be real where due to the mechanical loading of an elastic body, the strain causes a change in the temperature field. Moreover, the thermal conduction equation is of the parabolic type of the results of the propagation of thermal waves at an infinite speed, which also contradicts the real physical phenomena. Introduction of the strain rate term in the decoupled thermal conduction equation. The models of bodies explained the properties of the internal structure of medium when used the secondly law of thermodynamic with the development of semi-conductor integrated circuit

technology and solid-state sensors technology have been widely used in several fields. Previously, micro-mechanical structures of the thermo-elasticity and plasma field are analyzed experimental and theoretical as in Todorovic et al. [1-3]. Abbas et al. [4] presnted th solutions of photo-thermal interaction in a semiconducting materials with cylindrical hole and variable thermal conductivity. Hobiny and Abbas [5] discussed the photothermoelasticity interaction in a two-dimension semiconducting plane under Green-Naghdi theory. Lotfy et al. [6] studied the electro-magnetic and Thomson effects through the photo-thermal transport process of semiconductor material. Lotfy et al. [7] duscussed the responses of Thomson and electro-magnetic influnces of semi-conductor material casued by laser pulses under photo-thermoelastic excitation. Abbas et al [8] studied the analytical solution of plasma and thermo-elastic wave photogenerated by a focused laser beam in a semiconducting medium. Lotfy et al. [9] investigated the influnces of variable thermal conductivity in semiconductors mediums with cavity under fractional-order magneto-photothermal models. Alzahrani [10] investigated the effects of variable thermal conductivity in semi-conductor materiale. Alzahrani and Abbas [11] discussed the photothermoelasticity interactions in a two-dimentionn semiconductors mediums without energy dissipation. Hobiny and Abbas [12] presented a study on photo-thermal wave in an unbounded semiconductor material with cylindrical cavities. Das et al [13] studied the electro-magneto-thermo-elastic analysis for a thin circular semiconductor material.

The FDM is a numerical technique that finds an approximate solution of a given problem. The concept of this method is replacing the derivatives that appear in the differential equation by an algebraic approximation. The unknowns of the approximated algebraic equations are the dependent variables at the grid points. Mukhopadhyay and Kumar [14] applied the finite difference technique to study the generalized thermoelasticity problem of annular cylinders with variable material properties. Abd-Alla et al. [15] studied the effects in a thermoelastic annular cylinder using the finite difference method. Patra et al. [16] used the finite difference technique to study the computational model on thermoelastic analysis with the magnetic field in a rotating cylinder. Abd-Alla et al. [17] studied the effects of nonhomogeneous in an isotropic cylinder under magnetic field. Abd-Alla et al. [18] studied the solutions of the transient coupled thermoelastic of an annular fins by the implicit finite-difference technique. Many researchers [19-33] used the many thermoelasticity theories to get the solutions of many problems.

This investigation is an attempt to get new numerical solutions of photo-thermoelastic interactions in semiconductor medium by applying the implicit finite difference method (IFDM). Numerical outcomes for the carrier density, the displacement, the temperature and the redial and hoop stresses distributions are presented graphically. Finally, the accuracy of the finite difference method was validated by the comparing between the numerical and the analytical solutions for all physical fields.

2 Mathematical model

The governing formulations under the coupled photo-thermal theory for an isotropic semiconductor medium in the absence of the body force and the thermal source are presented as in [34-36]:

$$\mu u_{i,jj} + (\lambda + \mu) u_{j,ij} - \gamma_n N_{,i} - \gamma_t T_{,i} = \rho \frac{\partial^2 u_i}{\partial t^2} \tag{1}$$

$$D_e N_{,jj} - \frac{N}{\tau} + \frac{k}{\tau} T = \frac{\partial N}{\partial t}, \tag{2}$$

$$\left(K T_{,j}\right)_j + \frac{E_g}{\tau} N - \gamma_t T_o \frac{\partial u_{j,j}}{\partial t} = \rho c_e \frac{\partial T}{\partial t}. \tag{3}$$

$$\sigma_{ij} = \left(\lambda u_{k,k} - \gamma_t T - \gamma_n N\right)\delta_{ij} + \mu\left(u_{i,j} + u_{j,i}\right), \tag{4}$$

We consider an unbounded semiconducting material containing spherical cavities. Its state can be expressed in terms of the space variable r and the time t which occupying the region $a \leq r < \infty$. Due to symmetry involved in the problem, only the radial displacement $u_r = u(r,t)$ unvanishing, hence the formulations (1)-(4) are expressed as:

$$(\lambda + 2\mu)\left(\frac{\partial^2 u}{\partial r^2} + \frac{2}{r}\frac{\partial u}{\partial r} - \frac{2u}{r^2}\right) - \gamma_n \frac{\partial N}{\partial r} - \gamma_t \frac{\partial \Theta}{\partial r} = \rho \frac{\partial^2 u}{\partial t^2}, \tag{5}$$

$$D_e\left(\frac{\partial^2 N}{\partial r^2} + \frac{2}{r}\frac{\partial N}{\partial r}\right) - \frac{N}{\tau} + \frac{\delta}{\tau} T = \frac{\partial N}{\partial t}, \tag{6}$$

$$K\left(\frac{\partial^2 \Theta}{\partial r^2} + \frac{2}{r}\frac{\partial \Theta}{\partial r}\right) + \frac{E_g}{\tau} N = \rho c_e \frac{\partial \Theta}{\partial t} + \gamma_t T_o \frac{\partial}{\partial t}\left(\frac{\partial u}{\partial r} + \frac{2u}{r}\right), \tag{7}$$

$$\sigma_{rr} = (\lambda + 2\mu)\frac{\partial u}{\partial r} + \lambda \frac{2u}{r} - \gamma_n N - \gamma_t T. \tag{8}$$

$$\sigma_{\theta\theta} = \sigma_{\phi\phi} = (\lambda + 2\mu)\frac{u}{r} + \lambda\left(\frac{\partial u}{\partial r} + \frac{u}{r}\right) - \gamma_n N - \gamma_t T. \tag{9}$$

3 Initial and boundary conditions

In this problem, the initial conditions are given by

$$u(r,0) = 0, \frac{\partial u(r,0)}{\partial t} = 0, N(r,0) = 0, \frac{\partial N(r,0)}{\partial t} = 0, T(r,0) = 0, \frac{\partial T(r,0)}{\partial t} = 0, \tag{10}$$

While the boundary conditions can be given by

$$T(a,t) = T_1 e^{-\Omega t}, \tag{11}$$

$$D_e \frac{\partial N(r,t)}{\partial r}\Big|_{r=a} = s_b N(a,t)\,, \tag{12}$$

$$\sigma_{rr}(a,t) = 0, \tag{13}$$

Now, for appropriatenes, the dimensionaless physical fields can be given by

$$(r',u') = \omega c(r,u), (\sigma'_{rr},\sigma'_{\theta\theta}) = \frac{(\sigma_{rr},\sigma_{\theta\theta})}{\lambda+2\mu}, N' = \frac{N}{n_o}, (\mathrm{T}', T'_1) = \frac{(T,T_1)}{T_o}, \Omega' = \frac{\Omega}{\omega c^2}, (t',\tau') = \omega c^2(t,\tau) \quad , \tag{14}$$

where $\omega = \frac{\rho c_e}{K}$ and $c^2 = \frac{\lambda+2\mu}{\rho}$.

By using the variables of nondimensional forms (14), the basic relations with the neglecting of the dashes can be written by:

$$\frac{\partial^2 u}{\partial r^2} + \frac{2}{r}\frac{\partial u}{\partial r} - \frac{2u}{r^2} - a_2\frac{\partial T}{\partial r} - a_3\frac{\partial N}{\partial r} = \frac{\partial^2 u}{\partial t^2}, \tag{15}$$

$$\frac{\partial^2 N}{\partial r^2} + \frac{2}{r}\frac{\partial N}{\partial r} - \frac{a_4}{\tau}N + \frac{\beta}{\tau}T = a_4\frac{\partial N}{\partial t}, \tag{16}$$

$$\frac{\partial^2 \mathrm{T}}{\partial r^2} + \frac{2}{r}\frac{\partial T}{\partial r} + \frac{a_5}{\tau}N = \frac{\partial \mathrm{T}}{\partial t} + a_6\left(\frac{\partial^2 \mathrm{T}}{\partial r \partial t} + \frac{2}{r}\frac{\partial u}{\partial r}\right). \tag{17}$$

$$\sigma_{rr} = \frac{\partial u}{\partial r} + 2a_1\frac{u}{r} - a_2 T - a_3 N, \tag{18}$$

$$\sigma_{\theta\theta} = a_1\frac{\partial u}{\partial r} + (1+a_1)\frac{u}{r} - a_2 T - a_3 N, \tag{19}$$

$$T(a,t) = T_1 e^{-\Omega t}, \frac{\partial N(r,t)}{\partial r}\Big|_{r=a} = a_7 N(a,t), \sigma_{rr}(a,t) = 0, \tag{20}$$

where $a_1 = \frac{\lambda}{\lambda+2\mu}$, $a_2 = \frac{T_o\gamma_t}{\lambda+2\mu}$, $a_3 = \frac{n_o\gamma_n}{\lambda+2\mu}$, $\beta = \frac{\delta T_o}{n_o\omega D_e}$, $a_4 = \frac{1}{\omega D_e}$, $a_5 = \frac{n_o E_g}{\rho c_e T_o}$, $a_6 = \frac{\gamma_t}{\rho c_e}$, $a_7 = \frac{S_a}{\omega c D_e}$.

4 Analytical method

Applying the Laplace transforms for relations (15)-(20) are defined as

$$\bar{f}(r,p) = L[f(r,t)] = \int_0^\infty f(r,t)e^{-pt}dt\,, p > 0. \tag{21}$$

Hence, the following system are obtained

$$\frac{d^2\bar{u}}{dr^2} + \frac{2}{r}\frac{d\bar{u}}{dr} - \frac{2\bar{u}}{r^2} - a_2\frac{d\bar{T}}{dr} - a_3\frac{d\bar{N}}{dr} = p^2\bar{u}, \tag{22}$$

$$\frac{d^2\bar{N}}{dr^2} + \frac{2}{r}\frac{d\bar{N}}{dr} - a_4\frac{\bar{N}}{\tau} + \frac{\beta}{\tau}\bar{T} = pa_4\bar{N}, \tag{23}$$

$$\frac{d^2\bar{T}}{dr^2}+\frac{2}{r}\frac{d\bar{T}}{dr}+\frac{a_5}{\tau}\bar{N}=p\bar{T}+a_6p\left(\frac{d\bar{u}}{dr}+\frac{2\bar{u}}{r}\right), \tag{24}$$

$$\bar{\sigma}_{rr}=\frac{d\bar{u}}{dr}+a_1\frac{2\bar{u}}{r}-a_2\bar{T}-a_3\bar{N}, \tag{25}$$

$$\bar{\sigma}_{\theta\theta}=a_1\frac{d\bar{u}}{dr}+(1+a_1)\frac{\bar{u}}{r}-a_2\bar{T}-a_3\bar{N}, \tag{26}$$

$$\bar{T}(a,p)=\frac{T_1}{p+\Omega},\frac{d\bar{N}(r,p)}{dr}\Big|_{r=a}=a_7\bar{N}(a,p),\bar{\sigma}_{rr}(a,p)=0. \tag{27}$$

Differentiating Eqs (23) and (24) with respect to r and using in combination Eq. (22), which can be written as:

$$\frac{d^2\bar{u}}{dr^2}+\frac{2}{r}\frac{d\bar{u}}{dr}-\frac{2\bar{u}}{r^2}=p^2\bar{u}+a_2\frac{d\bar{T}}{dr}+a_3\frac{d\bar{\mathrm{N}}}{dr}, \tag{28}$$

$$\frac{d^2}{dr^2}\left(\frac{d\bar{N}}{dr}\right)+\frac{2}{r}\frac{d}{dr}\left(\frac{d\bar{N}}{dr}\right)-\frac{2}{r^2}\left(\frac{d\bar{N}}{dr}\right)=a_4\left(p+\frac{1}{\tau}\right)\frac{d\bar{N}}{dr}-\frac{\beta}{\tau}\frac{d\bar{\mathrm{T}}}{dr}, \tag{29}$$

$$\frac{d^2}{dr^2}\left(\frac{d\bar{\mathrm{T}}}{dr}\right)+\frac{2}{r}\frac{d}{dr}\left(\frac{d\bar{\mathrm{T}}}{dr}\right)-\frac{2}{r^2}\left(\frac{d\bar{\mathrm{T}}}{dr}\right)=p^3a_6\bar{u}+\left(pa_6a_3-\frac{a_5}{\tau}\right)\frac{d\bar{N}}{dr}+s(1+a_6a_2)\frac{d\bar{\mathrm{T}}}{dr}. \tag{30}$$

Now, it is possible to solve the coupled differential Eqs (28), (29) and (30) by the eigenvalues approaches proposed [37-41]. From Eqs. (38-30), the vector-matrix are written as

$$HV=AV, \tag{31}$$

where $H=\frac{d^2}{dr^2}+\frac{2}{r}\frac{d}{dr}-\frac{2}{r^2}$, $\mathrm{V}=\left[\bar{u}\quad\frac{d\bar{N}}{dr}\quad\frac{d\bar{T}}{dr}\right]^T$ and $A=\begin{bmatrix}a_{11}&a_{12}&a_{13}\\0&a_{22}&a_{23}\\a_{31}&a_{32}&a_{33}\end{bmatrix}$,

with $a_{11}=p^2,a_{12}=a_3,a_{13}=a_2\,,a_{22}=a_4\left(p+\frac{1}{\tau}\right),a_{23}=-\frac{\beta}{\tau},a_{31}=p^3a_6,$

$a_{32}=pa_6a_3-\frac{a_5}{\tau},a_{33}=p(1+a_6a_2).$

The matrix A has its characteristic formulation by

$$\eta^3-\eta^2(a_{22}+a_{33}+a_{11})-\eta(a_{23}a_{32}-a_{11}a_{33}-a_{22}a_{33}-a_{11}a_{22}+a_{13}a_{31})+a_{11}a_{23}a_{32}-a_{11}a_{22}a_{33}+a_{13}a_{22}a_{31}-a_{12}a_{23}a_{31}=0, \tag{32}$$

The eigenvalues of matrix A are the three roots of equation (32) which are named here η_1,η_2,η_3. Hence, the corresponding eigenvectors $X=[X_1,X_2,X_3]$ can be calculated as:

$$X_1=a_{13}(-\eta+a_{22})-a_{12}a_{23}\,,X_2=a_{11}a_{23}-\eta a_{23}\,,X_3-(\eta-a_{11})(\eta-a_{22}). \tag{33}$$

The solution of Eq. (31) which is bounded as $r\to\infty$ are expressed by

$$\bar{u}(r,p)=\sum_{i=1}^{3}A_iU_ir^{-1/2}K_{3/2}(m_ir), \tag{34}$$

$$\bar{N}(r,p)=-\sum_{i=1}^{3}A_iN_ir^{-1/2}K_{1/2}(m_ir), \tag{35}$$

$$\bar{T}(r,p) = -\sum_{i=1}^{3} A_i T_i r^{-1/2} K_{1/2}(m_i r), \tag{36}$$

where $m_i = \sqrt{\eta_i}$, $K_{3/2}$is the modified of Bessel's function of order $\frac{3}{2}$, $A_1, A_2$and $A_3$are constants that can be calculated by using the problem boundary conditions. The numerical inversion method adopted the final solutions of the temperature, the displacement, the carrier density and the stress distributions. The Stehfest approach [42] can be given by

$$f(x,t) = \frac{ln(2)}{t}\sum_{n=1}^{G} V_n \bar{f}\left(x, n\frac{ln(2)}{t}\right), \tag{37}$$

with

$$V_n = (-1)^{\left(\frac{G}{2}+1\right)} \sum_{p=\frac{n+1}{2}}^{min\left(n,\frac{G}{2}\right)} \frac{(2p)!p^{\left(\frac{G}{2}+1\right)}}{p!(n-p)!\left(\frac{G}{2}-p\right)!(2n-1)!},$$

where G is the term numbers

5 Numerical method

The basic relations obtained are linear partial differential equations. For the solutions problem, the implicit finite difference method (IFDM) is used. The solutions domain $0 \le t \le t_f, a \le r \le R_f$, are replaced by grids described by the set of nodes points (t_s, r_m), in which $t_s = sk, s = 0,1,2,\ldots\ldots,S$ and $r_m = mh,\ m = 0,1,2,\ldots\ldots,M$. Therefore, $k = \frac{t_f}{S}, h = \frac{r_f}{M}$ are taken as the time step and mess width respectively. For the time derivatives and the space derivatives, the derivatives are replaced the central differences. Thus, the approximations of finite difference method for the system of partial differential equations with respect to the independent variables:

$$\frac{\partial f}{\partial t} = \frac{f_m^{s+1} - f_m^{s-1}}{2k} + o(k^2), \frac{\partial^2 f}{\partial t^2} = \frac{f_m^{s+1} - 2f_m^{s} + f_m^{s-1}}{k^2} + o(k^2), \tag{38}$$

$$\frac{\partial f}{\partial r} = \frac{f_{m+1}^{s+1} - f_{m-1}^{s+1}}{2h} + o(h^2), \frac{\partial^2 f}{\partial r^2} = \frac{f_{m+1}^{s+1} - 2f_m^{s+1} + f_{m-1}^{s+1}}{h^2} + o(h^2), \tag{39}$$

The equations (15..19) are then replaced by the implicit finite difference equations by

$$\frac{u_{m+1}^{s+1} - 2u_m^{s+1} + u_{m-1}^{s+1}}{h^2} + \frac{u_{m+1}^{s+1} - u_{m-1}^{s+1}}{hr_m} - \frac{2u_m^{s+1}}{r_m^2} - a_2\frac{T_{m+1}^{s+1} - T_{m-1}^{s+1}}{2h} - a_3\frac{N_{m+1}^{s+1} - N_{m-1}^{s+1}}{2h} - \frac{u_m^{s+1} - 2u_m^{s} + u_m^{s-1}}{k^2} = 0, \tag{40}$$

$$\frac{N_{m+1}^{s+1} - 2N_m^{s+1} + N_{m-1}^{s+1}}{h^2} + \frac{N_{m+1}^{s+1} - N_{m-1}^{s+1}}{hr_m} - \frac{a_4}{\tau}N_m^{s+1} + \frac{\beta}{\tau}T_m^{s+1} - a_4\frac{N_m^{s+1} - N_m^{s-1}}{2k} = 0, \tag{41}$$

$$\frac{T_{m+1}^{s+1} - 2T_m^{s+1} + T_{m-1}^{s+1}}{h^2} + \frac{T_{m+1}^{s+1} - T_{m-1}^{s+1}}{hr_m} + \frac{a_5}{\tau}N_m^{s+1} - a_6\frac{u_{m+1}^{s+1} - u_{m+1}^{s-1} + u_{m-1}^{s+1} - u_{m-1}^{s-1}}{4hk} - 2a_6\frac{u_m^{s+1} - u_m^{s-1}}{2kr_m} - \frac{T_m^{s+1} - T_m^{s-1}}{2k} = 0, \tag{42}$$

$$\sigma_{rr} = \frac{u_{m+1}^{s} - u_{m-1}^{s}}{2h} + 2a_1\frac{u_m^s}{r_m} - a_2T_m^s - a_3N_m^s, \tag{43}$$

$$\sigma_{\theta\theta} = a_1\frac{u_{m+1}^{s} - u_{m-1}^{s}}{2h} + (1+a_1)\frac{u_m^s}{r_m} - a_2T_m^s - a_3N_m^s. \tag{44}$$

6 Numerical results and discussions

To make the full discussion for this phenomenon, the numerical simulation by using an element which belong to the semiconductor family. Therefore, the silicon (Si) material can be used as an example of semiconductor with physical constants of it. Si material has many applications in plasma modern physics and industrials technology. The physical constants in SI unit of photo-thermoelasticity of Si are given by the following [43]:

$T_o = 300(k), d_n = -9 \times 10^{-31}(m^3),\ \ \mu = 5.46 \times 10^{10}(N)(m^{-2}), \lambda = 3.64 \times 10^{10}(N)(m^{-2}),$
$E_g = 1.11\ (eV), \alpha_t = 3 \times 10^{-6}(k^{-1}),\ \ c_e = 695(J)(kg^{-1})(k^{-1}),\ \ \rho = 2330(kg)(m^{-3})x,$
$D_e = 2.5 \times 10^{-3}(m^2)(s^{-1}), s_b = 2\ (m)(s^{-1}), n_o = 10^{20}(m^{-3}), T_1 = 1, \tau = 5 \times 10^{-5}(s).$

The influence of the exponent of the decayed heat flux Ω in isotropic, linear semiconductors in the context of the coupled photo-thermoelastic theory are very important for researchers. The physical quantities in this problem subjected to the exponent of the decayed heat flux Ω are obtained graphically and discussed in 2D plotted which illustrated in Figures 1–5. The numerical techniques, outlined above, were used for the distributions of the temperature, the variation of redial displacement, the variation of carrier density, the variations of radial and hoop stresses with respect to the *r*-direction under coupled photo-thermal model. Figures 1 displays the temperature variation via the redial distance r. It is observed that the temperature equivalent to the constant temperature $T_1 = 1$ when $\Omega = 0$. While the temperature equal to $e^{-1.5*0.5} = 0.4724$ for $t = 0.5$ and $\Omega = 1.5$ which satisfy the problem boundary conditions on the internal surface of cavity $r = 1$ then the temperature decreases with the inncreasing of the redial distance r till it closes to zeros. Figure 2 show the carrier density variations via the radial distances r. It is notced that the carrier density start with its maxmum value on the internal surface of cavity $r = 1$ then the carrier density gradually decreases with the increasing of the redial distance r till it come to zeros values. Figures 3 depicts the displacement variations via the radial distance r. It is observed that the displacement attains maximum negative values then it increases gradually up to it attains a peak value at a particular location proximately close to the surface and then continuously decreases to zero. Figures 4 depict the redial stress variation via the redial distancee r. It is noticed that it start from zeros values which satisfied the problem boundary conditions. Figures 5 depict the hoop stress variations via the redial distancee r. It is oserved that the hoop stress attains some negative values then the magnitudes of stress decreases gradually to zeros values. The compressions between the solutions, one can conclude that considering the coupled photo-thermal model have major effects

on the physical quantities distributions. The increasing of the exponent of the decayed heat flux Ω reduces to the physical quantities magnitudes. Otherwise, figures 1-5 illustrates the solutions obtained numerically by the implicit finite difference method (IFDM) overlaid onto the solutions obtained analytically. The accuracy of the implicit finite difference method (IFDM) formulation was validated by comparing the analytical and numerical solutions for the field quantities.

Acknowledgments

This project was funded by the Deanship of Scientific Research (DSR) at King Abdulaziz University, Jeddah, under grant no. (G:104-130-1441). The authors, therefore, acknowledge with thanks DSR for technical and financial support.

Availability of Data and Material

There is no data or material that has been copied from elsewhere in the proposed manuscript.

Author Contributions

The authors have equal contribution in the paper.

Funding

This project was funded by the Deanship of Scientific Research (DSR) at King Abdulaziz University, Jeddah, under grant no. (G:104-130-1441).

Declarations

The authors declare that the manuscript follows ethical standards as per the guidelines provided during manuscript submission.

Conflict of Interest

The authors declare that there is no conflict of interest in the proposed manuscript as far as the publication is concerned.

Consent to Participate

There is mutual understanding between the two authors and is a combined work.

Consent for Publication

The authors have full faith on the publisher hence the publisher has full right for publication as per their guidelines.

References

1. Todorović, D (2003) Photothermal and electronic elastic effects in microelectromechanical structures. Review of scientific instruments, 74(1): 578-581.
2. Todorović, D (2003) Plasma, thermal, and elastic waves in semiconductors. Review of scientific instruments, 74(1): 582-585.
3. Song, Y, Cretin, B, Todorovic, DM, Vairac, P (2008) Study of photothermal vibrations of semiconductor cantilevers near the resonant frequency. Journal of Physics D: Applied Physics, 41(15): 155106.
4. Abbas, I, Hobiny, A, Marin, M (2020) Photo-thermal interactions in a semi-conductor material with cylindrical cavities and variable thermal conductivity. Journal of Taibah University for Science, 14(1): 1369-1376.
5. Hobiny, A, Abbas, I (2019) A GN model on photothermal interactions in a two-dimensions semiconductor half space. Results in Physics, 15): 102588.
6. Lotfy, K, El-Bary, A, Hassan, W, Alharbi, A, Almatrafi, M (2020) Electromagnetic and Thomson effects during photothermal transport process of a rotator semiconductor medium under hydrostatic initial stress. Results in Physics, 16): 102983.
7. Lotfy, K, Hassan, W, El-Bary, A, Kadry, MA (2020) Response of electromagnetic and Thomson effect of semiconductor medium due to laser pulses and thermal memories during photothermal excitation. Results in Physics, 16): 102877.
8. Abbas, IA, Aly, K, Dahshan, A (2018) Analytical solutions of plasma and Thermoelastic waves Photogenerated by a focused laser beam in a semiconductor material. Silicon, 10(6): 2609-2616.
9. Lotfy, K, El-Bary, A, Tantawi, R (2019) Effects of variable thermal conductivity of a small semiconductor cavity through the fractional order heat-magneto-photothermal theory. The European Physical Journal Plus, 134(6): 280.
10. Alzahrani, F (2020) The Effects of Variable Thermal Conductivity in Semiconductor Materials Photogenerated by a Focused Thermal Shock. Mathematics, 8(8): 1230.
11. Alzahrani, FS, Abbas, IA (2019) Photo-thermo-elastic interactions without energy dissipation in a semiconductor half-space. Results in Physics, 15): 102805.
12. Hobiny, AD, Abbas, IA (2017) A study on photothermal waves in an unbounded semiconductor medium with cylindrical cavity. Mechanics of Time-Dependent Materials, 21(1): 61-72.
13. Das, B, Ghosh, D, Lahiri, A (2021) Electromagnetothermoelastic analysis for a thin circular semiconducting medium. Journal of Thermal Stresses): 1-14.
14. Mukhopadhyay, S, Kumar, R (2009) Solution of a problem of generalized thermoelasticity of an annular cylinder with variable material properties by finite difference method. Computational Methods in Science and Technology, 15(2): 169-176.
15. Abd-Alla, AM, Abo-Dahab, SM, Kilany, AA) Finite difference technique to solve a problem of generalized thermoelasticity on an annular cylinder under the effect of rotation. Numerical Methods for Partial Differential Equations.
16. Patra, S, Shit, G, Das, B (2020) Computational model on magnetothermoelastic analysis of a rotating cylinder using finite difference method. Waves in Random and Complex Media): 1-18.
17. Abd-Alla, A, El-Naggar, A, Fahmy, M (2003) Magneto-thermoelastic problem in non-homogeneous isotropic cylinder. Heat and Mass transfer, 39(7): 625-629.

18. Abd-Alla, A, Salama, A, Abd-Ei-Salam, M, Hosham, H (2007) An implicit finite-difference method for solving the transient coupled thermoelasticity of an annular fin. Appl. Math. Inf. Sci, 1(1): 79-93.
19. Abbas, IA (2014) The effects of relaxation times and a moving heat source on a two-temperature generalized thermoelastic thin slim strip. Canadian Journal of Physics, 93(5): 585-590.
20. Zenkour, AM, Abbas, IA (2014) A generalized thermoelasticity problem of an annular cylinder with temperature-dependent density and material properties. International Journal of Mechanical Sciences, 84): 54-60.
21. Abbas, IA (2014) Nonlinear transient thermal stress analysis of thick-walled FGM cylinder with temperature-dependent material properties. Meccanica, 49(7): 1697-1708.
22. Lotfy, K (2019) Effect of variable thermal conductivity during the photothermal diffusion process of semiconductor medium. Silicon, 11(4): 1863-1873.
23. Lotfy, K, Abo-Dahab, S, Tantawy, R, Anwar, N (2019) Thermomechanical Response Model on a Reflection Photothermal Diffusion Waves (RPTD) for Semiconductor Medium. Silicon): 1-11.
24. Hobiny, A, Abbas, I (2019) Fractional Order GN Model on Photo-Thermal Interaction in a Semiconductor Plane. Silicon): 1-8.
25. Abbas, IA, Marin, M (2017) Analytical solution of thermoelastic interaction in a half-space by pulsed laser heating. Physica E: Low-dimensional Systems and Nanostructures, 87): 254-260.
26. Riaz, A, Ellahi, R, Bhatti, MM, Marin, M (2019) Study of heat and mass transfer in the Eyring–Powell model of fluid propagating peristaltically through a rectangular compliant channel. Heat Transfer Research, 50(16.
27. Bhatti, M, Ellahi, R, Zeeshan, A, Marin, M, Ijaz, N (2019) Numerical study of heat transfer and Hall current impact on peristaltic propulsion of particle-fluid suspension with compliant wall properties. Modern Physics Letters B, 33(35): 1950439.
28. Marin, M, Vlase, S, Ellahi, R, Bhatti, MM (2019) On the partition of energies for the backward in time problem of thermoelastic materials with a dipolar structure. Symmetry, 11(7): 863.
29. Itu, C, Öchsner, A, Vlase, S, Marin, MI (2019) Improved rigidity of composite circular plates through radial ribs. Proceedings of the Institution of Mechanical Engineers, Part L: Journal of Materials: Design and Applications, 233(8): 1585-1593.
30. Marin, M, Ellahi, R, Chirilă, A (2017) On solutions of Saint-Venant's problem for elastic dipolar bodies with voids. Carpathian journal of Mathematics, 33(2): 219-232.
31. Marin, M (2010) Lagrange identity method for microstretch thermoelastic materials. Journal of Mathematical Analysis and Applications, 363(1): 275-286.
32. El-Naggar, A, Kishka, Z, Abd-Alla, A, Abbas, I, Abo-Dahab, S, Elsagheer, M (2013) On the initial stress, magnetic field, voids and rotation effects on plane waves in generalized thermoelasticity. Journal of Computational and Theoretical Nanoscience, 10(6): 1408-1417.
33. Palani, G, Abbas, I (2009) Free convection MHD flow with thermal radiation from an impulsively-started vertical plate. Nonlinear Analysis: Modelling and Control, 14(1): 73-84.
34. Song, Y, Bai, J, Ren, Z (2012) Study on the reflection of photothermal waves in a semiconducting medium under generalized thermoelastic theory. Acta Mechanica, 223(7): 1545-1557.
35. Mandelis, A, Nestoros, M, Christofides, C (1997) Thermoelectronic-wave coupling in laser photothermal theory of semiconductors at elevated temperatures. Optical Engineering, 36(2): 459-468.
36. Youssef, HM, El-Bary, AA (2018) THEORY OF HYPERBOLIC TWO-TEMPERATURE GENERALIZED THERMOELASTICITY. Materials Physics and Mechanics, 40): 158-171.
37. Das, NC, Lahiri, A, Giri, RR (1997) Eigenvalue approach to generalized thermoelasticity. Indian Journal of Pure and Applied Mathematics, 28(12): 1573-1594.

38. Abbas, IA (2014) Eigenvalue approach in a three-dimensional generalized thermoelastic interactions with temperature-dependent material properties. Computers & Mathematics with Applications, 68(12): 2036-2056.
39. Abbas, IA (2014) Eigenvalue approach for an unbounded medium with a spherical cavity based upon two-temperature generalized thermoelastic theory. Journal of Mechanical Science and Technology, 28(10): 4193-4198.
40. Abbas, IA (2015) A dual phase lag model on thermoelastic interaction in an infinite fiber-reinforced anisotropic medium with a circular hole. Mechanics Based Design of Structures and Machines, 43(4): 501-513.
41. Abbas, IA (2015) The effects of relaxation times and a moving heat source on a two-temperature generalized thermoelastic thin slim strip. Canadian Journal of Physics, 93(5): 585-590.
42. Stehfest, H (1970) Algorithm 368: Numerical inversion of Laplace transforms [D5]. Communications of the ACM, 13(1): 47-49.
43. Song, Y, Todorovic, DM, Cretin, B, Vairac, P, Xu, J, Bai, J (2014) Bending of Semiconducting Cantilevers Under Photothermal Excitation. International Journal of Thermophysics, 35(2): 305-319.

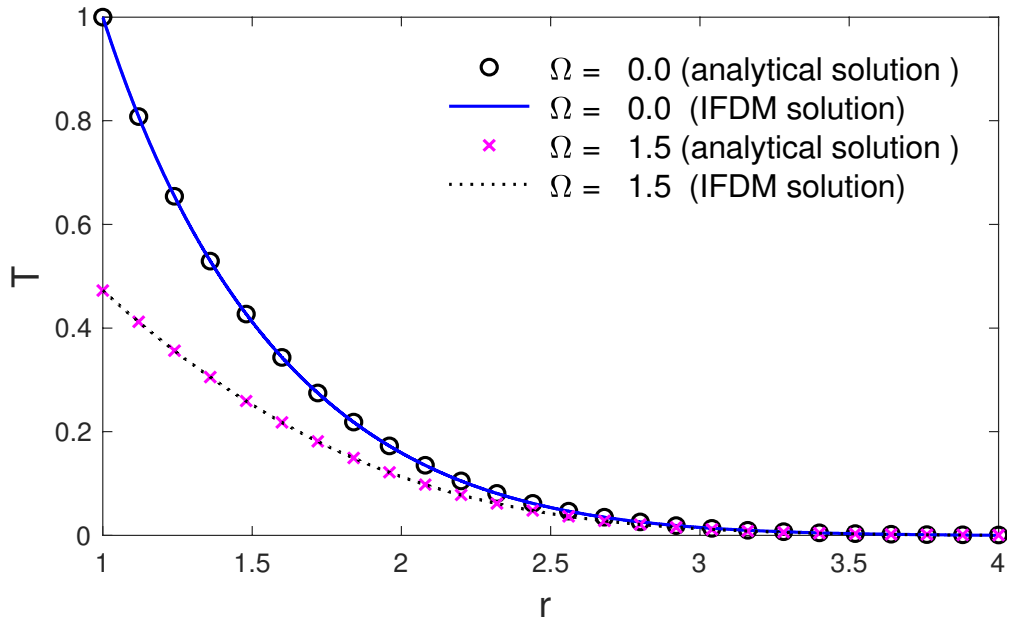

Fig. 1 The temperature variation via the distance with and without the exponent of the decayed heat flux Ω.

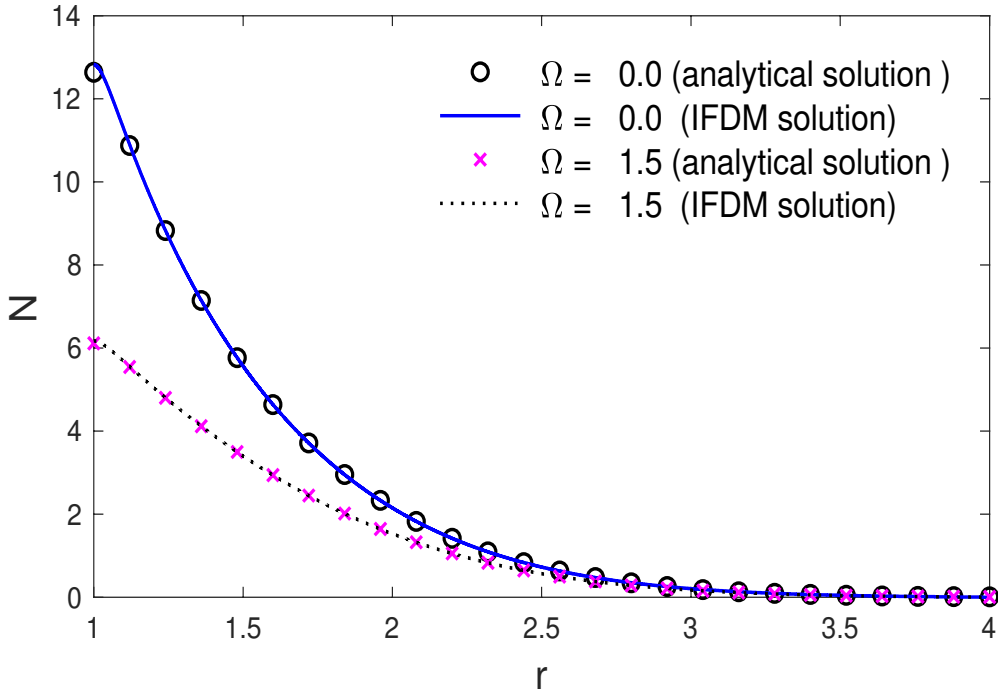

Fig. 2 The carrier density variation via the distance with and without the exponent of the decayed heat flux Ω.

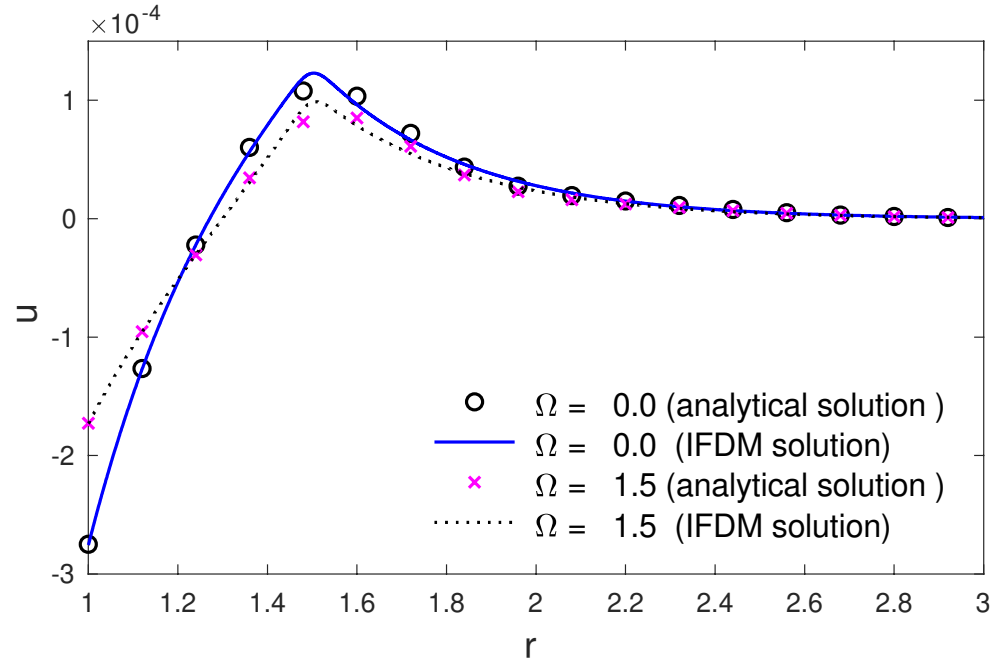

Fig. 3 The redial displacement variations via the distances with and without the exponent of the decayed heat flux Ω.

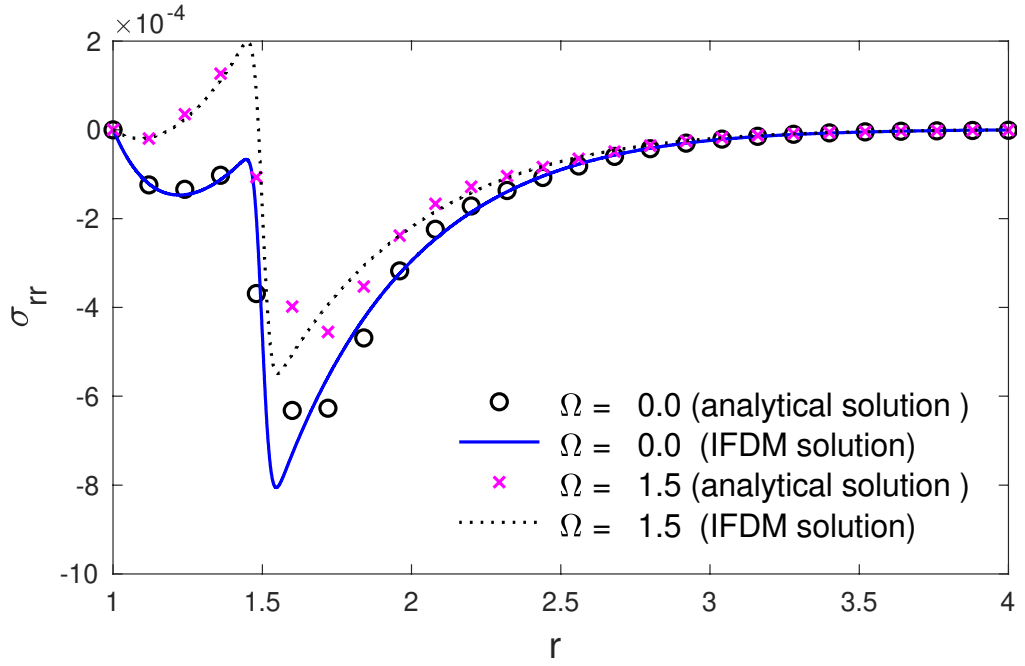

Fig. 4 The redial stress variations via the distance with and without t

he exponent of the decayed heat flux Ω.

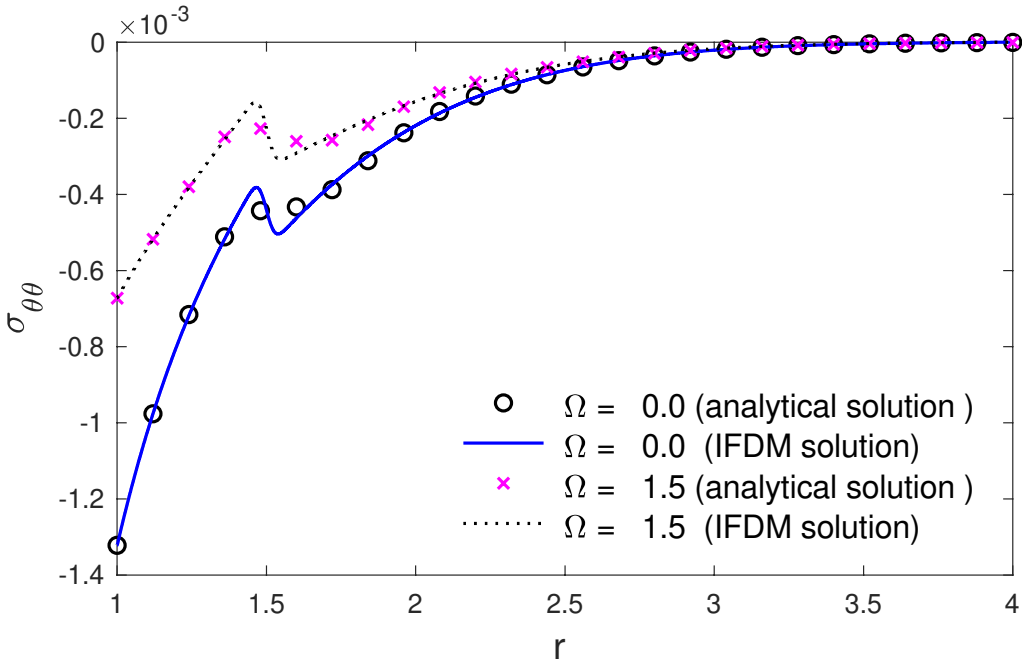

Fig. 5 The hoop stress variations via the distance with and without

the exponent of the decayed heat flux Ω.

Figures

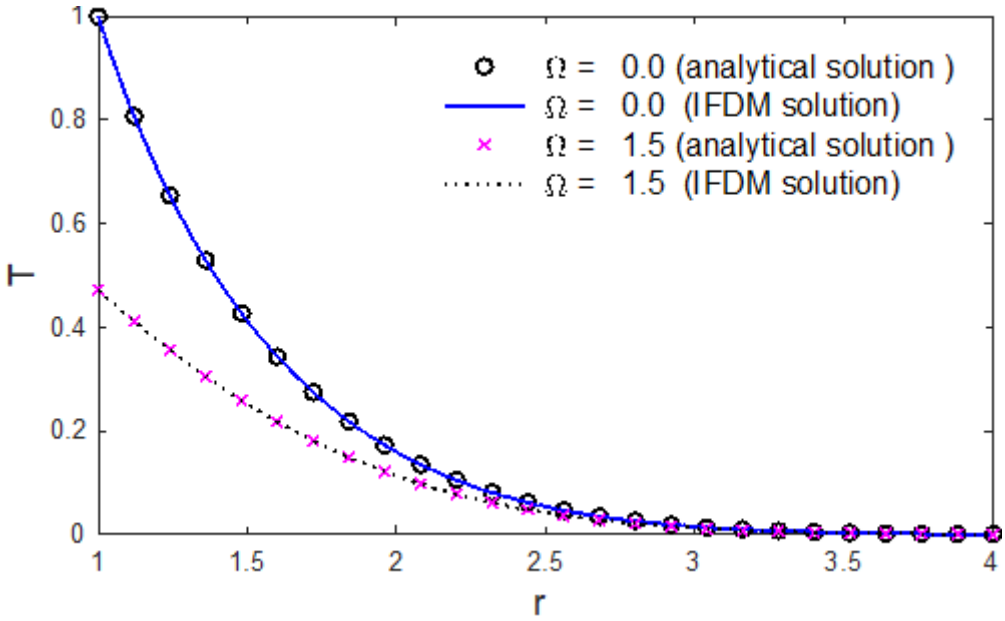

Figure 1

The temperature variation via the distance with and without the exponent of the decayed heat flux Ω.

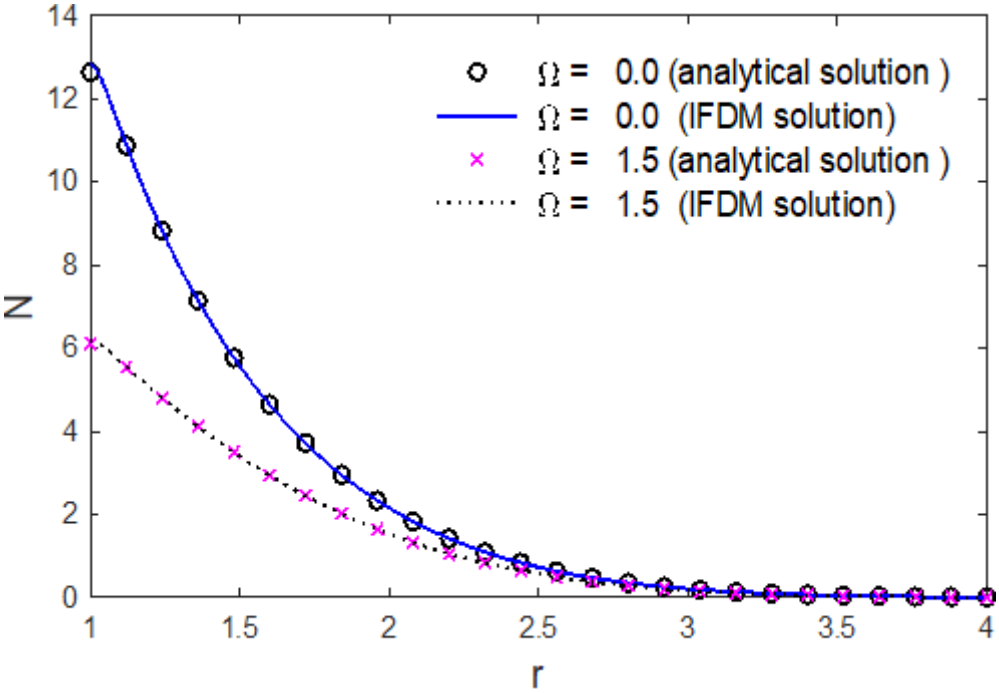

Figure 2

The carrier density variation via the distance with and without the exponent of the decayed heat flux Ω.

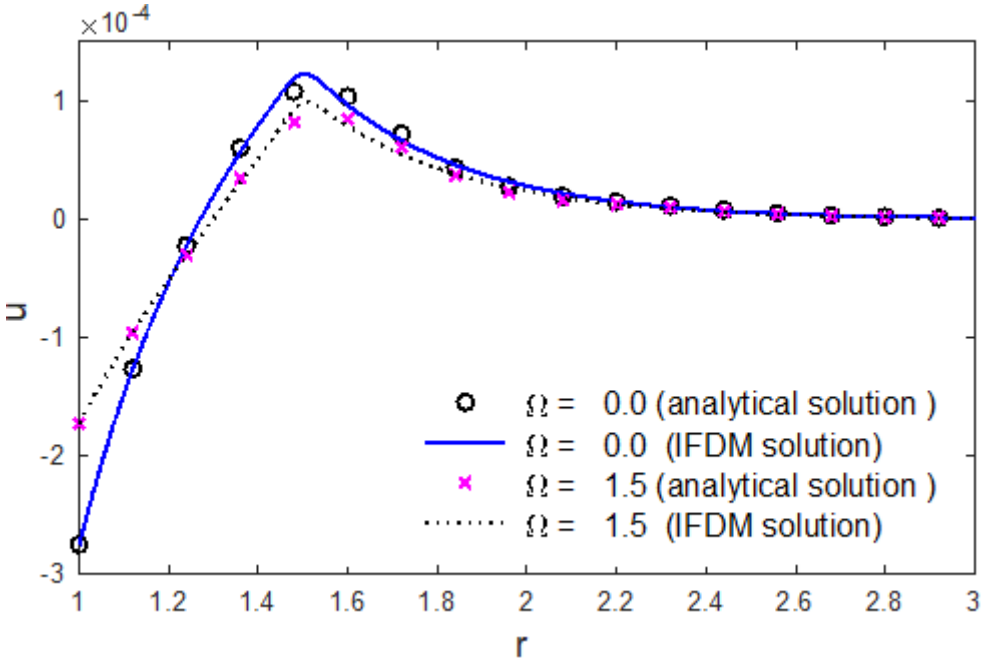

Figure 3

The redial displacement variations via the distances with and without the exponent of the decayed heat flux Ω.

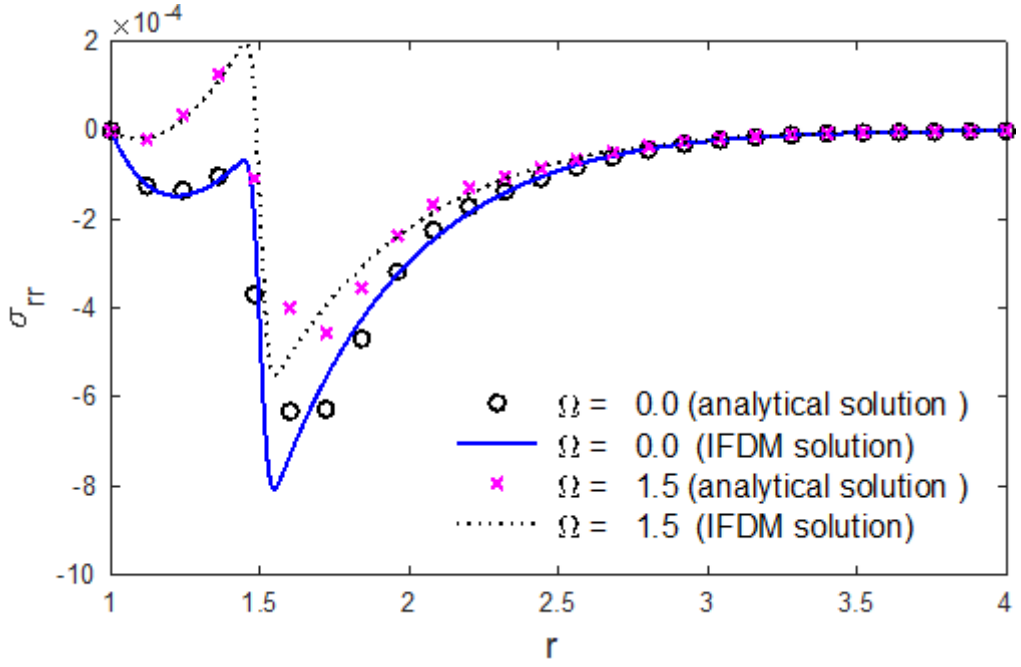

Figure 4

The redial stress variations via the distance with and without t he exponent of the decayed heat flux Ω.

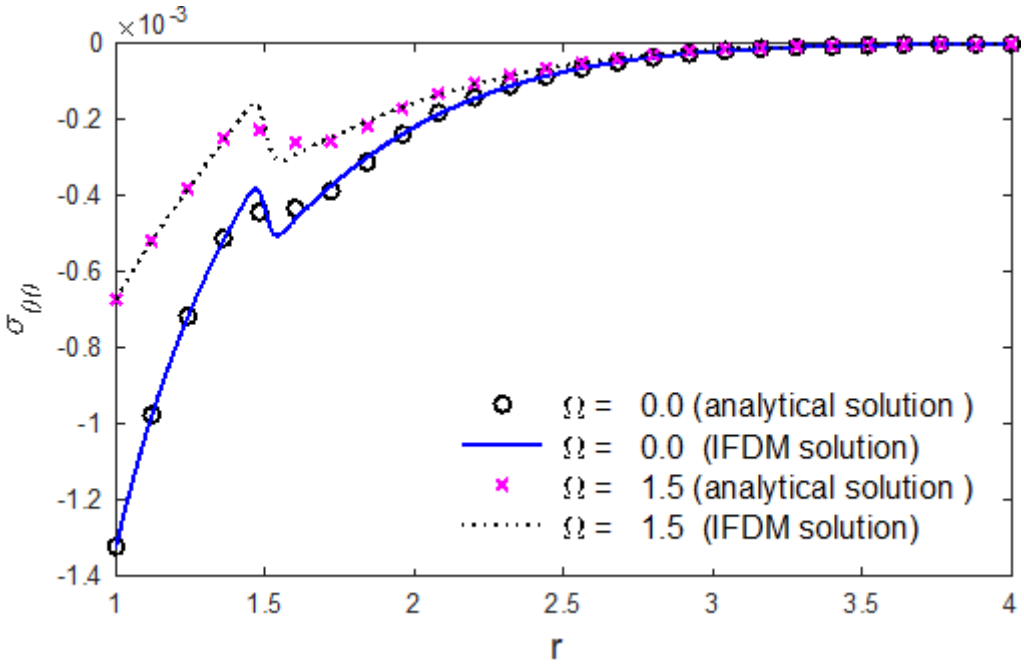

Figure 5

The hoop stress variations via the distance with and without the exponent of the decayed heat flux Ω.